Journal of Statistical Physics, Vol. 86, Nos. 5/6, 1997

The Granular Phase Diagram

Sergei E. Esipov[1] and Thorsten Pöschel[2]

Received August 1, 1996

The kinetic energy distribution function satisfying the Boltzmann equation is studied analytically and numerically for a system of inelastic hard spheres in the case of binary collisions. Analytically, this function is shown to have a similarity form in the simple cases of uniform or steady-state flows. This determines the region of validity of hydrodynamic description. The latter is used to construct the phase diagram of granular systems and discriminate between clustering instability and inelastic collapse. The molecular dynamics results support analytical results, but also exhibit a novel fluctuational breakdown of mean-field descriptions.

KEY WORDS: Granular hydrodynamics; Boltzmann equation; granular temperature.

Granular media such as sand provide an attractive opportunity to revisit a number of topics in classical physics and contribute new angles of view. In this paper we describe the granular phase diagram, which we hope will be helpful to a broad community, given the rising interest in granular systems.[1] Researchers interested in diluted granular gases, such as in astrophysical applications,[2] and researchers who study, say, compaction of sand[3] use different approaches. The phase diagram may represent a ground for communication.

The phase of a granular system depends on the inelasticity of collisions r (restitution coefficient approximation[4–6]), particle density ρ, particle size a, system size L, and observation time t. The external influence of shaking, gravity, boundaries enters through the above parameters. Neither

[1] James Franck Institute and Department of Physics, University of Chicago, Chicago, Illinois 60637.

[2] Institute für Physik, Humboldt-Universität zu Berlin, D-10015, Berlin, Germany.

0022-4715/97/0300-1385$12.50/0 © 1997 Plenum Publishing Corporation

granular temperature nor any other characteristic of the rate of bulk-averaged motion appears on the phase diagram, since there is no characteristic energy scale for hard-core interaction assumed here. As we shall see below, the combination $\rho L a^{d-1}$, where d is the system dimension, plays the key role. It represents the average number of particles inside an imaginary tube of length L and cross section a^{d-1}. The phase diagram consists of at least three regions (Fig. 1). In the region $1-r \ll (\rho L a^{d-1})^{-2}$ the system is gaslike. In the region $(\rho L a^{d-1})^{-2} \ll 1-r \ll (\rho L a^{d-1})^{-1}$ the system is condensed, but does not collapse, and for $(\rho L a^{d-1})^{-1} \ll 1-r$ the system contains inelastically collapsed chains of particles mixed with noncollapsing regions (see ref. 7 for the description of collapse).

Figure 2 is a snapshot from a two-dimensional event-driven molecular dynamics (MD) with 5000 particles in a circle the wall of which is maintained at a constant temperature. Particles undergo inelastic collisions with a constant coefficient of restitution [see Eqs. (3) and (4) below]. When a particle hits the wall it experiences diffusive angular scattering, while the distribution of the scattered velocity amplitude is Maxwellian, with the temperature being that of the wall. After a period of equilibration the system finds the state drawn in Fig. 2, which is in many respects a steady state. In Fig. 2 the gray scale linearly codes the relative number of collisions experienced by each particle during the previous 10^5 time steps, where black means high collision rate. One can clearly distinguish three different regions: (i) close to the wall there is a gaslike phase with low density, where the mean free path is large. (ii) The region between the center of the bulk and the wall consists of closely packed particles. We consider this region as the condensed phase. It is well separated from the gaslike phase. (iii) Close to the center of the container we find a region which is not

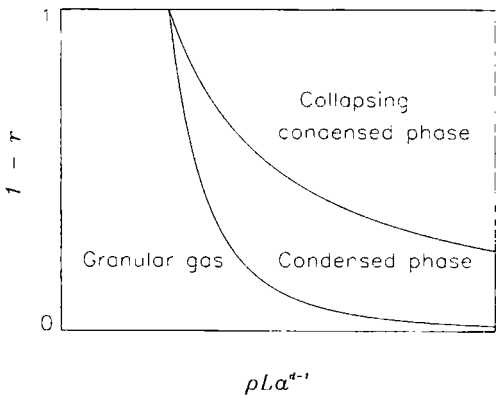

Fig. 1. The granular phase diagram. See text for details.

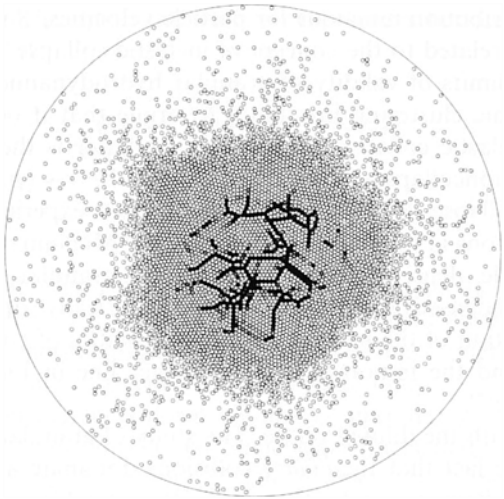

Fig. 2. A snapshot from an event-driven molecular dynamics simulation of 5000 hard spheres. The wall is kept at a fixed temperature. The gray scale codes the relative number of collisions experienced by particles during the previous 10^5 time steps. One distinguishes three regions: a gaslike state with low density, and two high-density regions, with and without collision chains (cf. Fig. 1).

distinguishable from the second region by the naked eye. With the help of gray scale coding one observes collision chains, i.e., almost linearly arranged chains of particles which make a major contribution to the previous 10^5 collisions in comparison to their neighbors.

Quantitatively, about 5% of the particles participate in about 96% of the collisions. Sometimes we observe that very few ($\approx$5–10) particles make almost all of the collisions in a certain time interval (not shown). The lengths of the appearing chains as well as their lifetimes vary irregularly; their statistics will be discussed in detail elsewhere.[8] Figure 2 serves as an illustration that in MD simulation one encounters all three regions of the phase diagram given in Fig. 1.

The role of observation time is not included here, and will be discussed separately below. Notwithstanding this classification, the condensed phases may be ordered in space (a crystal) or disordered (a glass). This different structure-based classification exists in the elastic limit. We now present the arguments used for constructing Fig. 1 beginning from the gaslike phase.

As the parameter $\rho L a^{d-1}$ increases, the first condensation or clustering transition of granular gas occurs. The above criterion was obtained by Goldhirsch and Zanetti[6] with the use of granular hydrodynamics.[4, 5] This description is based on the assumption of molecular chaos[9] and

Maxwellian distribution functions for particle velocities,[4] which have been questioned and related to the concept of inelastic collapse.[10] In this paper we present the limits of validity of granular hydrodynamics, and then use the hydrodynamic clustering instability to argue that it occurs before the condition of inelastic collapse is satisfied. The latter is the line separating collapsing and noncollapsing condensed phases, $1-r \sim (\rho L a^{d-1})^{-1}$.[7, 10], [3]

Inelastic collapse, when a chain of particles experiences an infinite number of collisions in finite time as discussed by McNamara and Young,[7] is realized inside dense clusters, specified by granular hydrodynamics. Inside such condensed regions we have numerically observed *collision* chains. The relation of the hydrodynamic instabilities of collision chains to their collapse and the importance of the upper line in Fig. 1 will be discussed elsewhere[8].

We begin with the diluted phase. The study of granular gases is greatly simplified by the fact that the *binary* collisions dominate and goes back to the work of Boltzmann and others.[11, 9] It is unclear *a priori* whether inelasticity represents a regular or a singular perturbation. The first part of this problem is the reduction of the Boltzmann equation to hydrodynamics; it can be studied independent of the known complications associated with hydrodynamic description, i.e., divergence of transport coefficients at high orders in spatial inhomogeneities and in low dimensions.[12] The situation is somewhat analogous to the kinetics of phonons, where hydrodynamic reduction and second sound have a restricted range of applicability as compared to the kinetic equation.[13] A more difficult problem is the validity of the Boltzmann equation itself, or the hypothesis of molecular chaos.

The Boltzmann equation for inelastically colliding identical particles reads[11, 9, 14]

$$\partial_t f + \mathbf{v}\,\partial_{\mathbf{x}} f = \hat{C}(f, f) \tag{1}$$

where $f(\mathbf{v}, \mathbf{x}, t)$ is the velocity distribution function and $\hat{C}$ is the bilinear collision operator

$$\hat{C}(f, f) = \int \left\{ \frac{1}{r^2} f_1' f' - f f_1 \right\} |\mathbf{v} - \mathbf{v}_1|\, d\sigma\, d\mathbf{v}_1 \tag{2}$$

The differential cross section of two spheres of radius a is $d\sigma = \pi a^2 \sin^2\theta\, d\theta/2$, where θ is the angle between the vectors $\mathbf{q}$ and $\mathbf{v}-\mathbf{v}_1$. An

[3] The 1D model used in ref. 10 is a degenerate one, where any distribution function is an integral of motion in the dilute limit. Additional study shows that it is sufficient to introduce internal degrees of freedom to recover hydrodynamics even in one dimension.

incoming collision event to the state $\{\mathbf{v}, \mathbf{v}_1\}$ occurs between particles with velocities $\mathbf{v}'$ and $\mathbf{v}_1'$,

$$\mathbf{v}' = \mathbf{v} - \frac{1+r}{2r}\mathbf{q}[\mathbf{q}\cdot(\mathbf{v}-\mathbf{v}_1)] \tag{3}$$

$$\mathbf{v}_1' = \mathbf{v}_1 - \frac{1+r}{2r}\mathbf{q}[\mathbf{q}\cdot(\mathbf{v}-\mathbf{v}_1)] \tag{4}$$

where $\mathbf{q}$ is a unit vector pointing from the center of the sphere 1 to the center of the sphere 2, and $0 < r < 1$ is the so-called coefficient of restitution; it models energy losses in the center-of-mass reference frame.[7, 15] In the case $r = 1$ one recovers the usual elastic limit.

We now consider a uniform cooling of granular gas without gravity inside an elastic two-dimensional circle when inelasticity is too small for developing clustering instability.[6] The problem is (hopefully!) isotropic and homogeneous and the distribution function f_0 must depend only on the absolute value of particle velocity v i.e., on kinetic energy, $E = mv^2/2$. When the initial distribution is forgotten one may search for a similarity solution

$$f_0(E, t) = \frac{n}{T(t)}\phi\left(\frac{E}{T(t)}\right) \tag{5}$$

where $T(t)$ is a single scale of the kinetic energy. The normalization condition to the number density of particles n is $\int dz\phi(z) = 1$. Equations (1) and (2) result in an integrodifferential equation for the function $\phi(z)$

$$\begin{aligned} -A(r)\left(\frac{d}{2}\phi + z\frac{d\phi}{dz}\right) &= \sqrt{2}\int d\alpha\, dz_1\, d\sigma g(z_1) \\ &\times \left\{\frac{1}{r^2}\phi_1'\phi' - \phi\phi_1\right\}(z - z_1 - \sqrt{zz_1}\cos\alpha)^{1/2} \end{aligned} \tag{6}$$

and in an equation for $T(t)$,

$$dT/dt = -A(r)\, T^{3/2} \tag{7}$$

Here $A(r)$ is the constant introduced by separation of variables, α is the angle between vectors $\mathbf{v}$ and $\mathbf{v}_1$, and $g(z)$ is the density of states. Examination of the collision integral allows one to get the asymptotic form of $\phi(z)$ at large z. Namely, it can be shown that the incoming term contains extra

factor $O(z^{-1/2})$ [this is contributed by the events $(\mathbf{qv}) \propto z^{-1/2}$] and is small as compared to the outgoing term. The asymptotic form of Eq. (6) is $-A(r)\, z(d\phi/dz) \sim \phi z^{1/2}$, up to a number. Therefore,

$$\ln \phi(z) \sim \sqrt{z}/A(r) \tag{8}$$

The moments of this function converge, and one can restrict oneself to the hydrodynamic description (7) of the granular temperature, which gives

$$T(t) = T_0 \left[1 + \frac{t}{2} A(r) \sqrt{T_0} \right]^{-2} \tag{9}$$

and $T(t) \propto t^{-2}$ at large t.[5] One can get this power law from dimensional arguments. $A(r)$ remains undetermined; it can only be found from the full solution of Eq. (6). Asymptotically, $A(r) \propto (1-r)$ when r is close to 1. The enhanced population of large energies, (8), dominates at $z \gg 1/A^2(r)$. For lower energies the distribution is Maxwellian.

Two sets of MD results by an event-driven code are obtained with 5000 (20,000) particles of unit radius in a circle with radius 130 (260). In both cases the surface fraction covered by particles is 50/169. Units of mass, length, and time are arbitrary, and the initial velocity distribution is taken to be uniform in velocity in the square $-1 \leqslant v_x, v_y \leqslant 1$. The employed model of collision is the same as given above, $r = 0.999$. Figure 3

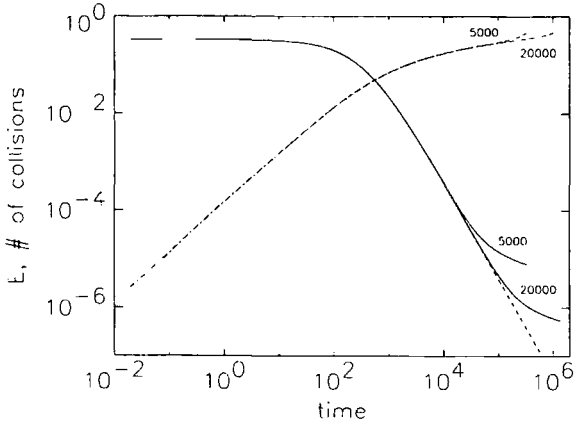

Fig. 3. The kinetic energy E per particle over time t from MD simulations. Energy decay curves for systems with 5000 and 20,000 particles are identical for a very long time (solid lines). The dashed line shows the prediction of Eq. (8) with $T_0 = 0.333$ and $A = 0.01$. The dash-dotted lines display the cumulative number of collisions per particle scaled by factors 10^{-8} (5000) and 4×10^{-8} (20,000).

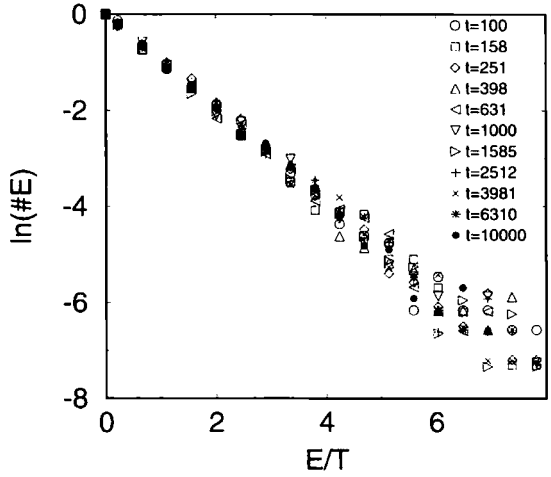

Fig. 4. Evolution of the scaled energy distribution function in MD simulations. Different symbols are used for different times as shown. Statistically, the distribution is indistinguishable from Maxwellian within the given range.

shows the temporal evolution of mean kinetic energy and the number of collisions occurred. The fit to the energy decay over the entire range is achieved with the help of Eq. (9). The distribution function is self-similar over four orders of energy decay, as is seen in Fig. 4. This figure shows the energy distribution function with the argument rescaled by $\langle E(t)\rangle = T$ for different times. One can see that the hydrodynamic description is quite precise. The system remains uniform and gaslike.

However, at times $t \sim 10^4$–10^5 we observed appearance of a rarefied space in the center of the circle followed by "condensation" of granular gas on the wall. This is a novel type of transition, which is different from clustering[6] or collapse.[7] One can understand the growth of fluctuations using the following argument. The mean free path l is given by $l = 1/n\sigma = a/c$ with the volume fraction $c = na^d$ in a d-dimensional system with concentration n. The diffusivity of particles decreases in time like $D(t) \sim (\delta v)\, l \sim l\sqrt{T}$, where T is given in energy units. At large t [Eq. (9)],

$$T = \frac{4}{(tA)^2} \sim \left[\frac{l}{t(1-r)}\right]^2 \tag{10}$$

Therefore,

$$D \sim \frac{l^2}{t(1-r)} = \frac{(a/c)^2}{t(1-r)} \tag{11}$$

and the diffusion length of particles in time t is

$$l_D \sim \sqrt{\int D(t)\,dt} \sim \frac{(a/c)^2}{1-r} \ln^{1/2}\left(\frac{tv_0}{a}\right) \tag{12}$$

where v_0 is the typical initial velocity. The number of particles inside the sphere of radius l_D is $N \sim nl_D^d = c(l_D/a)^d$. These particles preserve a fluctuational collective velocity $v_0[c(l_D/a)^d]^{1/2}$. Equating this velocity to thermal velocity $\delta v \sim \sqrt{T(t)} \sim (a/c)/[t(1-r)]$ yields the time when the collective velocity exceeds the fluctuational individual velocity δv,

$$t_c \sim \frac{a}{v_0} \frac{c^{(d-3)/2}}{(1-r)^{(4+d)/4}} \ln^{-d/4}\left(\frac{c}{1-r}\right) \tag{13}$$

given with logarithmic precision. Granular flow becomes fluctuationally *supersonic* at $t \gg t_c$ and the molecular chaos assumption along with the Boltzmann equation and granular hydrodynamics are no longer applicable. The r.h.s. of Eq. (13) can be evaluated, and the corresponding time is 5.0×10^4. Given that the numerical prefactor in the estimate (13) is not known, one finds a very satisfactory agreement between the estimate (13) and the time where hydrodynamic prediction deviates from the MD time trace of kinetic energy density in Fig. 3. At time t_c groups of particles of the size $l_c \sim [\int^{t_c} dt\, D(t)]^{1/2}$ become special. Their mutual encounters lead to structures containing traveling *shock waves*. The difference between the systems with 5000 and 20,000 particles as seen in Fig. 3 is due to the fact that the regions of the size l_c occupy a different fraction of the area, and in the second case it takes longer for inhomogeneities to evolve from the size l_c up to the system size. The observed fluctuational transition is the reason why observation time may explicitly appear in the phase diagram.

We now add a constant energy supply from the border and allow the system to reach a steady state. The system is no longer uniform in space, and we assume that the corresponding length scales exceed the mean free path l everywhere. The similarity Ansatz (5) with a nonuniform temperature $T(x)$ can be used again. A study of the asymptotic form of the collision term shows that in the regions of the phase space where the detailed balance is absent the incoming term is again small in $O(z^{-1/2})$ times as compared to the outgoing term, and no global balance is possible. If $1-r \ll 1$, the detailed balance approximately holds for the energies, $z \ll (1-r)^{-1}$, above this range there are effectively no particles. Therefore,

we find that the distribution function is almost Maxwellian for the energies less than $T/(1-r)$ and small otherwise,

$$\phi(z) = \begin{cases} e^{-z} & z \ll (1-r)^{-1} \\ 0, & z \gg (1-r)^{-1} \end{cases} \tag{14}$$

All the moments converge, and one can justify the hydrodynamic reduction, which reads[4, 6, 10]

$$\nabla P(\rho, T) = 0 \tag{15}$$

$$\nabla q - B(r)\, T/\tau_c(\rho, T) = 0 \tag{16}$$

where P is the granular pressure and q is the thermal flux.[4, 16] This system can be analyzed. To understand what happens as one increases inelasticity (or the number of particles), it is useful to consider the dilute limit approximation when $q = \lambda(T)\nabla T$, $P = \rho T$, where $\lambda(T) = \gamma_1 T^{1/2}$ is the thermal conductivity, and $B(r) \propto (1-r)$ is the energy fraction lost per collision. $\tau_c^{-1}(n, T) = \gamma_2 \rho T^{1/2}$ is the time between collisions. We found that the hydrodynamic solution exists only below a threshold,

$$a^{d-1} B^{1/2}(r) \int_0^L \rho\, dx < \xi_d(\gamma_1/\gamma_2) \ln(L/a) \tag{17}$$

ξ_d is a pure number. Our hydrodynamic analysis is valid when (17) is fulfilled; in the opposite case a particle condensate appears, and system has more than one phase. The left-hand side of (17) is the generalization of the parameter $\rho L a^{d-1}$ for the nonuniform case. Its region of applicability is more general than the derivation given above. Equation (17) describes with logarithmic precision the same clustering transition as discussed by Goldhirsch and Zanetti.[6]

Returning to the question of the validity of the hydrodynamic reduction of the Boltzmann equation, we note that the complete system of equations for granular hydrodynamics[17, 4, 16] for density, linear and angular velocity, and granular temperature(s) has a shortcoming. It follows from Eqs. (8), (14) that in sufficiently inelastic complex flows where changes occur in space and time the granular temperature cannot be introduced. Indeed, if we restricted ourselves to the first moment of the energy distribution in situations when this distribution changes its functional form, we would not be able to close the hydrodynamic reduction. Therefore, in general, the full system of hydrodynamic equations[17, 4] cannot serve as a quantitative description. The situation is a bit easier, though, than in the kinetics of phonons: only kinetic coefficients are not exact, and the

uncertainty is in numerical prefactors, which depend on the local distribution function. To give an example about the difficulties with phonons it is sufficient to recall that the heat transfer may be nonlocal.[18]

Sufficiently inelastic problems require a mixed kinetic–hydrodynamic description. In this case, similar to the kinetics of phonons,[18] one finds a reduced kinetic equation for the isotropic part f_0 of the distribution function

$$\partial_t f_0 - \nabla \mathbf{J}[f_0] = \hat{C}(f_0, f_0) \tag{18}$$

where the diffusionlike flux $\mathbf{J}$ is defined as

$$\mathbf{J}(f) = \frac{4E}{9m}\left[\frac{\delta \hat{C}}{\delta f}\right]^{-1} \nabla f \tag{19}$$

The inverse integral operator $[\delta \hat{C}/\delta f]^{-1}$ is fixed by particle number constraint, i.e., the result of applying this operator to f_0 must have vanishing norm. Similar expressions arise for all dissipative coefficients. Despite the cumbersome appearance, Eq. (18) together with the remaining hydrodynamic equations for density and momentum conservation offers a reduction from nine- to five-dimensional space of arguments.

Our study of an inelastic gas with binary collisions has provided an opportunity to justify granular hydrodynamics for simple flows and for all flows in dilute and sufficiently elastic systems. This allows one to discriminate between clustering instability discussed by Goldhirsch and Zanetti[6] and inelastic collapse.[7] In complex inelastic flows the predictions of granular hydrodynamics are valid in order of magnitude almost everywhere, and such precision is comparable to that in Fig. 1. On the basis of this study we constructed the granular phase diagram and identified a novel type of supersonic fluctuational phase transition, leading to shock waves, which is different from clustering and collapse.

ACKNOWLEDGMENTS

We acknowledge the constant interest of H. Jaeger and discussions with other members of the Chicago Sand Club, Y. Du, E. Grossman, L. Kadanoff, S. Nagel, C. Salueña, and T. Zhou. We thank P. Chaikin, R. Jackson, R. Lieske, L. Schimansky-Geier, and F. Spahn for useful discussions. S.E.E. is indebted to D. Frenkel for saving a copy of ref. 11 from being trashed at the Physics Library of the University of Illinois at Urbana-Champaign. This work was supported in part by the MRSEC Program of the National Science Foundation under the grant DMR9400379.

REFERENCES

1. R. P. Behringer, *Nonlinear Sci. Today* **3**:2 (1993); H. Jaeger, S. Nagel, and R. P. Behringer, to be published.
2. H. A. Weaver and L. Danly, eds., *The Formation and Evolution of Planetary Systems* (Cambridge University Press, Cambridge, 1989).
3. J. K. Knight, C. G. Fandrich, C. N. Liu, H. M. Jaeger, and S. R. Nagel, *Phys. Rev. E* **51**:3957 (1995).
4. C. K. K. Lun and S. B. Savage, *J. Appl. Math.* **54**:47 (1987).
5. P. K. Haff, *J. Fluid Mech.* **134**:401 (1983); *J. Rheol.* **30**:931 (1986).
6. I. Goldhirsch and G. Zanetti, *Phys. Rev. Lett.* **70**:1619 (1993).
7. S. McNamara and W. R. Young, *Phys. Rev. E* **50**:R28 (1994).
8. S. E. Esipov and T. Pöschel, Unpublished.
9. E. M. Lifshitz and L. P. Pitaevskii, *Physical kinetics* (Pergamon Press, New York, 1981).
10. Y. Du, H. Li, and L. P. Kadanoff, *Phys. Rev. Lett.* **74**:1268 (1995).
11. L. Boltzmann, *Vorlesungen über Gastheorie*, ed. J. A. Barth (Leipzig, 1923).
12. Y. Pomeau and P. Résibois, *Phys. Rep.* **19**:63 (1975).
13. V. L. Gurevich, *Kinetika Fononnyh Sistem* (Nauka, Moscow, 1982); *Transport in Phonon Systems* (North-Holland, Amsterdam, 1986).
14. A. Isihara, *Statistical Physics* (Academic Press, New York, 1971).
15. S. McNamara, Ph.D. Thesis, Scripps Institute of Oceanology, San Diego, California (1995).
16. C.-H. Wang, R. Jackson, and S. Sundaresan, *J. Fluid Mech.* (1996), in press, and references therein.
17. S. R. de Groot and P. Mazur, *Non-equilibrium Thermodynamics* (Dover, New York, 1981), pp. 304–311.
18. Y. B. Levinson, *Zh. Eksp. Teor. Fiz.* **79**:1394 (1980); *Sov. Phys. JETP* **52**:704 (1980); S. E. Esipov and Y. B. Levinson, *Pis'ma Zh. Eksp. Teor. Fiz.* **34**:218 (1981); *JETP Lett.* **34**:210 (1981).

Communicated by D. Stauffer